

An Evaluation of Thermosyphon Heat Pipe Charged R134a and R600a Using Machine-Learning Algorithms

Rini Hannah G¹ and R. S. Anand^{2*}

¹Independent Researcher, Kanyakumari, TN, India

²Guangzhou Institute of Energy Conversion, Chinese Academy of Sciences, Guangzhou, China

ABSTRACT

Thermosyphon Heat Pipe (THP) is a heat transfer device that consists of three sections with working fluid inside, including evaporator, adiabatic, and condenser. The refrigerants in thermosyphons are commonly used for low-temperature applications. In this article, two higher heat transfer refrigerants, namely R600a and R134a, are used as the working fluid in thermosyphon to compare their performance. The total thermal resistance of the refrigerant R600a and R134a charged thermosyphon was calculated using experimental results, and it shows that R600a provides lower thermal resistance than R134a. Experimental results show that the heat transfer of R600a increases by 12% than R134a. The temperature at the evaporator and condenser section provides the performance of the thermosyphon. Therefore, in addition to the experimental results, three different machine-learning methods such as support vector machine supporting vector machine (SVM), artificial neural network artificial neural networks (ANN) and convolutional neural network Convolution Neural Network (CNN) are deployed to classify the efficiency of the experimental process and find the accuracy of the output using these methods. These approaches are used to diagnose the temperature with the input parameters such as the ratio between length to diameter, condenser to evaporator length, thermal conductivity of working fluid, boiling point of working fluid, temperature of the cooling water, applied heat flux and heat input. The neural schema applied over the measured temperature obtained from the experimental results was optimized with the algorithmic approach which provides the relative grade. In this article, the classifiers are used to compare the performance of the refrigerants and measure the accuracy of the evaluation for R600a and R134a.

Keywords: cylindrical thermosyphon, two-phase heat transfer, neural network, prediction, thermal resistance

Correspondence concerning this article should be addressed to R. S. Anand, Guangzhou Institute of Energy Conversion, Chinese Academy of Sciences, Guangzhou, China, E-mail: anand_rs@outlook.com

Competing interests: We declare that there are no conflicts of interest.

Received:10-AUG-2024. Revised: 19-FEB-2025. Accepted &Published: 23-FEB-2025.

INTRODUCTION

Refrigerant is a fluid for which the phase change happens at low temperatures. Refrigerants are necessary for various fields like scientific research, space technology, refrigeration systems, blood preservation, medicine, food, and so on (Abas et al., 2018; Celen et al., 2014; Kasaeian et al., 2018). The refrigerant in a thermosyphon is utilized for low-temperature applications in which the thermosyphon material and working fluid play a significant role (Jafari et al., 2016; Zhang et al., 2018).

To identify the compatibility and heat transportation capability with refrigerants in thermosyphon, many researchers have been carried out with the inclination angle and fill ratios. The thermal performance of

thermosyphon is studied by Ong et al. (2016) with different fill ratios and inclination angles using R410a refrigerant for varying heat inputs ranging from 40W to 100W. The experiment result shows no significant impact on the filling ratio and inclination angle. Anand et al. (2020) evaluated the thermosyphon's performance using a low global warming potential refrigerant HFE7000. The experimentation is conducted for different inclination angles and includes nanoparticles in refrigerants for varying heat input between 30W and 150W. The outcome of the investigation reveals that the HFE7000 can also transfer heat for different inclinations of thermosyphon. Also, it is noticed that the inclination impacts the performance of the thermosyphon. Ong and Haider-e-Alahi (2003) evaluate thermosyphon performance using R134a as a working fluid. The result reveals that an increase in fill ratio, mass flow rate of the coolant, and temperature difference between the evaporator and condenser increases the performance of the thermosyphon. The working fluids such as R134a, R22, water, and ethanol are experimented with in a thermosyphon by Payakaruk et al. (Payakaruk et al., 2000). In this experiment, fill ratio, aspect ratio, and inclination angle are the major parameters considered. The experiment showed no effect on the filling ratio of 50, 80, or 100% with the heat transfer of the thermosyphon. The above works in the literature show that refrigerants are suitable for heat transfer applications. However, the effects of the inclination angle mentioned by the researchers were found to be opposite.

Alongside, certain works in the literature state that refrigerants are also used in the modified thermosyphon for inclined heat transfer appliances and the enhancement of the heat transfer. Sukchana and Pratinthong (Sukchana & Pratinthong, 2016) brought a flexible Teflon® hose in the adiabatic section of the thermosyphon for inclined heat transfer using R134a. Experiments were carried out for different tilt angles and bending radii by applying various heat fluxes at the evaporator section. The experimental analysis shows that the optimum tilt angle of 45% achieved better results for the entire tilting and bending angle with the flexible hose thermosyphon. The flexible hose in the adiabatic section of the thermosyphon is recommended for heat transfer in inaccessible electronic systems. Naresh and Balaji (2018) used an internal finned condenser with R134a as a working fluid to evaluate the thermal performance of the thermosyphon. The analysis is done by varying the mass flow rate of the cooling water, fill ratios, and different heat inputs. The study divulges an increase of 13% in condensation heat transfer in the thermosyphon, and the fill ratio is also decreased by using an internal fin in the condenser section. Hence, the literature suggests that refrigerants are suitable for any means of thermosyphon for heat transfer applications.

The thermosyphon refrigerant is suitable for low heat transfer applications; hence, researchers seek further to identify the better heat transfer refrigerant among many refrigerants. Gorecki (2018) investigated the thermosyphon's performance using refrigerants such as R134a, R440a, and R470c for different fill ratios. The experiment concluded that R134a and R440a produced high heat transfer for a fill ratio of 10% while R470c generated 50% less heat transfer than the other two refrigerants. An experimental analysis is conducted by Limin Ma et al. (Ma et al., 2017) on eight hydrocarbon and freon refrigerants in thermosyphon for renewable energy applications. This shows that refrigerant R134a performs better than other pure refrigerants.

Furthermore, the recent advancement in thermosyphon focused on the optimization and prediction of performance using artificial neural networks, machine learning, and deep learning techniques. Maleki et al. (2021) predicted the performance of thermosyphon using artificial neural networks (ANN) for the nanofluid-charged thermosyphon. The temperature distribution and the inflow and outflow water temperature around the condenser were determined using the Levenberg Marquardt algorithm. The ANN predicted result shows good agreement with the experimental result, and the comparison result obtained between them achieves the root square value of 0.99. Using the rules in fuzzy logic and active learning algorithms, the thermal efficiency of the multi-walled carbon nanotube with silver nanofluid and multi-walled carbon nanotube without silver was optimized by Shanbedi et al. (Shanbedi et al., 2015). The predicted thermal efficiency was in good agreement with the experimental result. The prediction of oscillating behavior on the loop thermosyphon is done by Fichera and Pagano (2002). The neural

network-based nonlinear moving average of autoregressive models was used to find the dynamic behavior inside it. This study inferred that the neural network-based approach could give step-forward predictions even in the absence of suitable governing equations.

The above works inferred from the literature show that refrigerant plays a significant role in heat transportation for low-temperature applications in thermosyphon. However, the effect of the inclination angle on performance is contradictory in the research fraternity. Moreover, among all the refrigerants, R134a and R600a have the highest heat transfer capability in thermosyphon.

This study addresses two critical aspects of thermosyphon heat pipe (THP) research: First, it employs machine learning algorithms, including Support Vector Machine (SVM), Convolutional Neural Network (CNN), and Artificial Neural Network (ANN) approaches, along with mathematical models, to predict THP performance. Second, it compares R134a and R600 refrigerants in THP, with particular attention to inclination angle effects. This research represents the first comprehensive application of machine learning algorithms for thermosyphon performance prediction, offering a novel approach that can evaluate performance without requiring extensive experimental procedures.

EXPERIMENTAL STUDIES AND PROCEDURES

Fabrication of THP

A copper pipe of 12.7 mm diameter and a total length of 315 mm is chosen by splitting 90, 90, and 135 mm for the evaporator, adiabatic, and condenser segments, respectively. To make it a closed tube, two end caps are made in which a filling tube is brazed in one end cap for charging the working fluid. The cleaning process removes foreign particles and dust in the copper tube and end cap using deionized water and a deoxidizing solution. The end cap without the filling tube is brazed at the evaporator end, and the end cap with the filling tube is brazed into the condenser end of the copper tube. A thermocouple of T-type is employed at each section of the THP to measure the temperature response at each section. Two thermocouples are employed at the evaporator section with a length of 15 mm (T1) and 75 mm (T2), respectively.

Table 1: Properties of the Refrigerant R134a and R600a

Refrigerant	ODP	GWP	Boiling point (°C)	Critical temperature (°C)	Critical pressure (MPa)	Flammability	Safety class from ASHRAE
R134a	nil	1300	-26.1	101	4.05	nonflammable	A1 (i.e., low toxicity and nonflammable)
R600a	nil	0	-11.6	134.7	3.64	flammable	A3 (i.e., highly flammable)

Abbreviations: ASHRAE American society of Heating, Refrigeration and Air-Conditioning, GWP global warming potential, ODP ozone depletion potential.

At the adiabatic section two thermocouples are fixed at a length of 105 mm (T3) and 165 mm (T4) from the bottom. Three thermocouples are placed at the condenser section at a length of 195 mm (T5), 247.5 mm (T6) and 315 mm (T7) respectively. The acrylic tube chamber is made around the condenser section for condensation with the inlet and outlet. The thermocouples are also fixed at the water inlet (T8) and outlet (T9) to find the heat output in the THP. The working fluids are charged inside it through the filling tube, and then the valve is closed after the required amount of working fluid is filled. The properties of charged working fluid are represented in Table 1. In this experiment, the entire evaporator section is filled with the working fluid as per the suggestions by the past research works. For the heating purpose at the evaporator section, a nichrome wire of flat type is equally wended over it. During experiments, the THP is insulated by means of fiberglass wool, to reduce heat loss with the surroundings.

Experimental Test Rig

The experiment test rig is shown in Figure 1 which has three units namely, heating unit, cooling unit and the temperature recording unit.

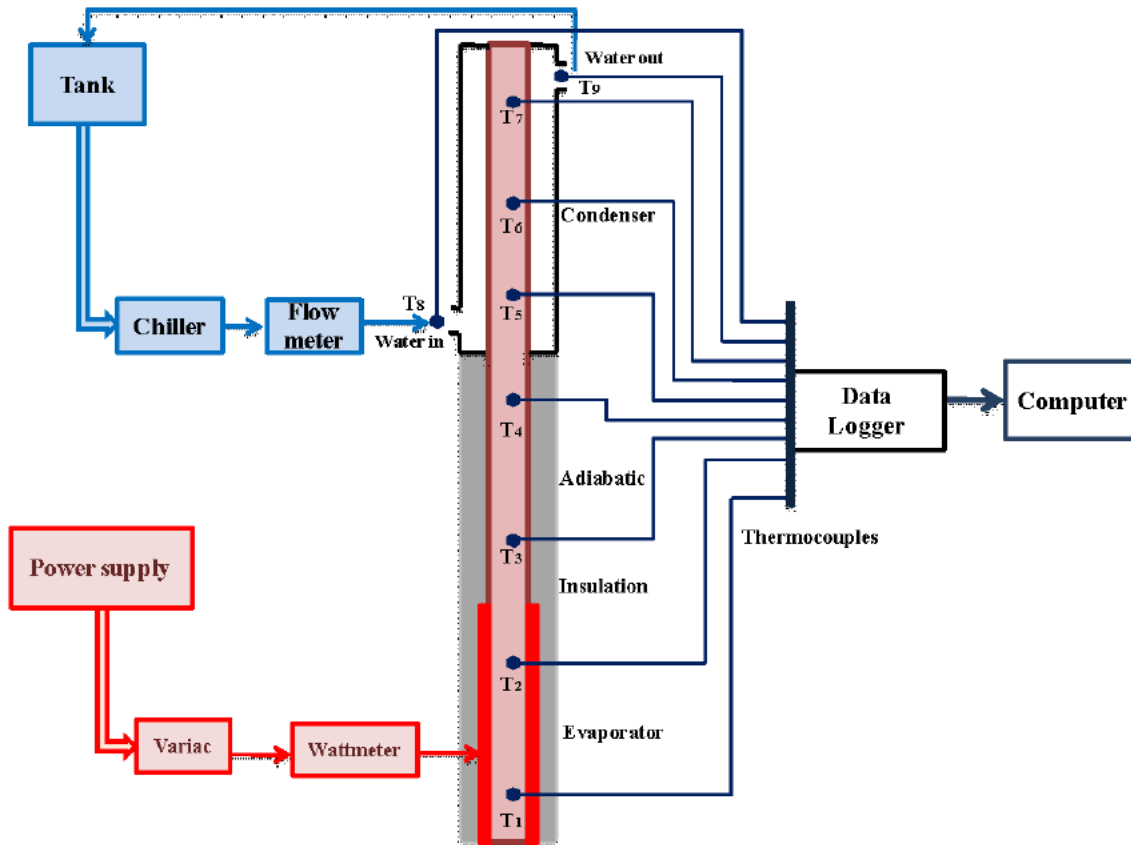


Figure 1. Experimental setup of thermosyphon

The heating unit consists of a wattmeter and variac. When the power supply is turned on, the variac supplies only the required current to the evaporator's heating element. The wattmeter shows the amount of current in Watts. The cooling unit has a chiller and flowmeter. The required temperature (i.e., 12 °C) and the flow rate can be maintained using the chiller and flowmeter, respectively. The temperature recording unit has a data logger and a computer. The thermocouples (T1—T9) are fixed into the data logger, and the temperature response can be monitored and recorded using the computer. The uncertainty in the flow rate and temperature are $\pm 3\%$ and $\pm 0.1\%$. The uncertainty in the data logger with the thermocouple is ± 0.2 °C.

Data Reduction

The temperatures obtained at the THP, power supply, and water inlet and outlet from the condenser are the primary parameters of the data reduction process.

The heat input and the output can be calculated by

$$Q_{in} = V.I \quad (1)$$

$$Q_{out} = m_l C_{pl}(T_9 - T_8) \quad (2)$$

where Q_{in} and Q_{out} are the heat input and heat output at the evaporator and condenser sections, respectively. V is the voltmeter, and I is the ammeter readings. m is the mass flow rate; C_{pl} is the heat capacity of water, and $T_9 - T_8$ is the temperature difference between the outlet and inlet water temperature around the condenser.

The overall thermal resistance of the THP can be obtained using the below equation.

$$R_{all} = \frac{\Delta T}{Q_{out}} \quad (3)$$

Where, R_{all} is the overall resistance of the THP, ΔT is the mean temperature difference between the evaporator and condenser section. The thermal resistance at the evaporator and condenser section can be calculated using the equation

$$R_{eve} = \frac{\Delta T_{eve}}{Q_{in}} \quad (4)$$

$$R_{con} = \frac{\Delta T_{con}}{Q_{out}} \quad (5)$$

Where R_{eve} and R_{con} are the evaporator and condenser thermal resistance. ΔT_{eve} is the temperature difference between the evaporator mean temperature ($T_1 + T_2/2$) and vapour temperature (T_3). ΔT_{con} is the temperature difference between the vapour temperature (T) and condenser mean temperature ($T_5 + T_6 + T_7/3$).

Heat transfer rate at the evaporator and the condenser can be calculated by the following equations

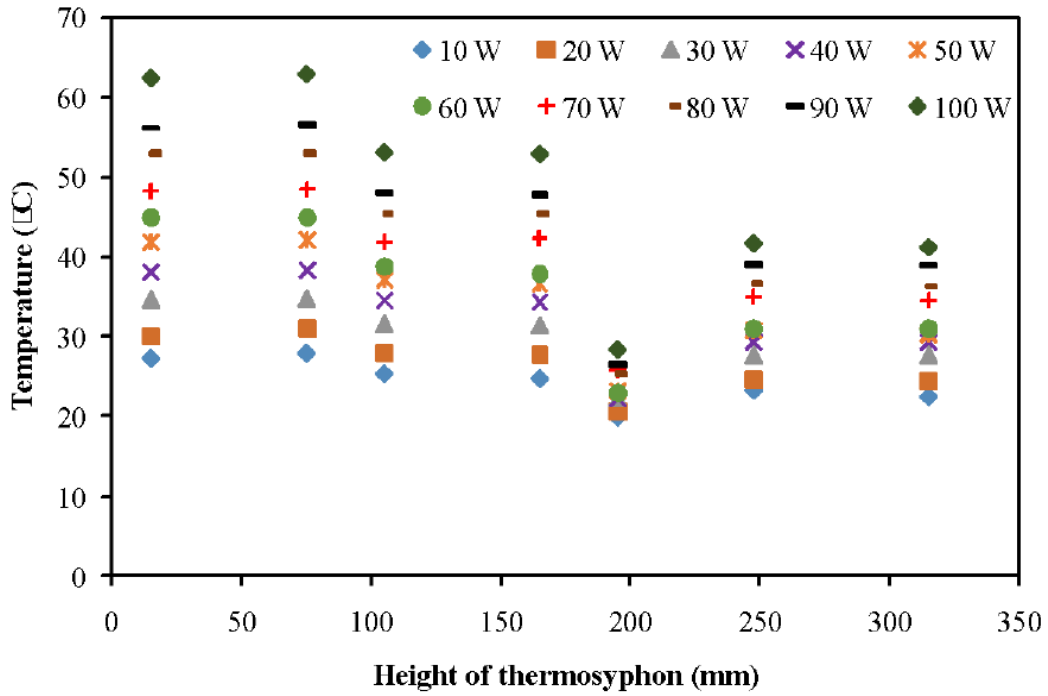
$$h_e = \frac{Q_{in}}{\pi d l_{eve} \Delta T_{eve}} \quad (6)$$

$$h_c = \frac{Q_{out}}{\pi d l_{con} \Delta T_{con}} \quad (7)$$

where, h_e and h_c are the heat transfer coefficient at the evaporator and condenser sections respectively; and ΔT_{eve} is the temperature difference between the evaporator mean temperature ($T_1 + T_2/2$) and vapor temperature (T_3). ΔT_{con} is the temperature difference between the vapor temperature (T_4) and condenser mean temperature ($T_5 + T_6 + T_7/3$).

RESULTS AND DISCUSSION

(A)



(B)

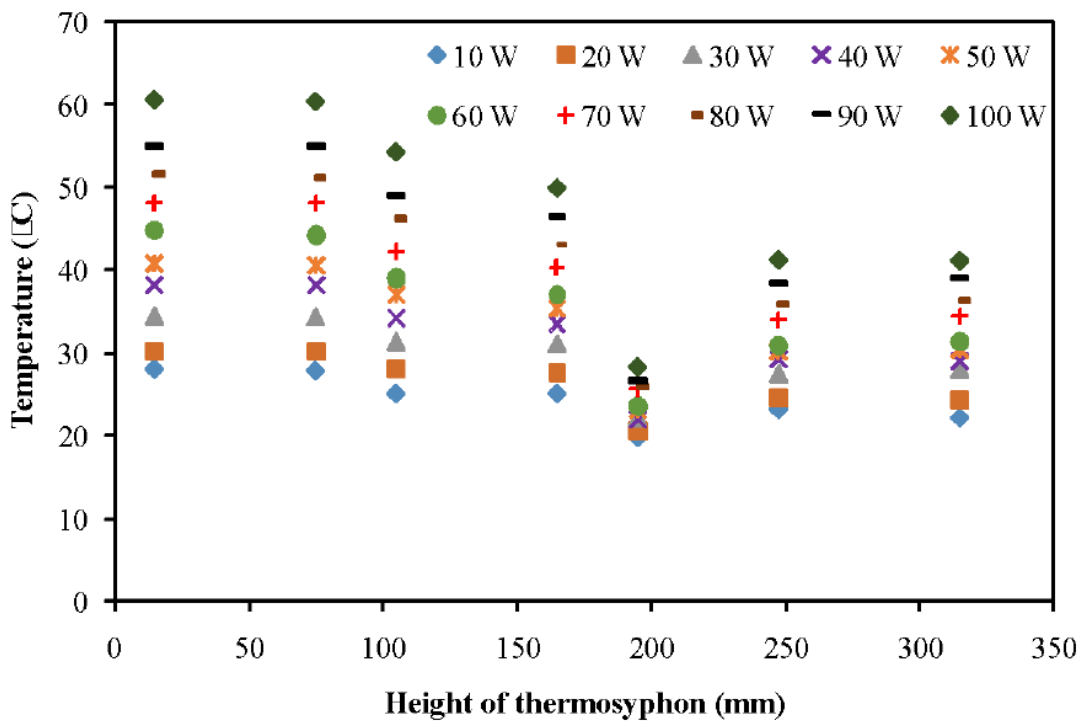


Figure 2. Temperature at the thermocouple fixed position of the thermosyphon for applied heat input (A) R134a and (B) R600a

The THP charged R600a and R134a are analyzed with the applied heat input of 10W—100W at the evaporator section. The temperature response of each section for the TPH with the applied heat input is shown in Figure 2. It is noticed that the temperature of the experimented THP increases with an increase in heat input from 10 W to 100 W.

The temperature output obtained in this experiment for the applied heat input gives a similar trend of the past researchers. The temperature at the section of evaporator is higher than the section of adiabatic and condenser, which is due to the heat applied in that section. It is observed from Figure 2a, 2b, one thermocouple fixed at the condenser (195 mm) shows very less temperature which is due to the entry of cooling water at that region as shown in the experimental setup (Figure 1). It is also shown that the temperatures obtained for the sections for R134a charged THP are slightly higher than R600a charged THP. The mean difference in temperature between R134a and R600a charged THP is 2.3, 1.1 and 0.4 °C at the sections of evaporator, adiabatic and condenser respectively for higher heat input (i.e., 100 W).

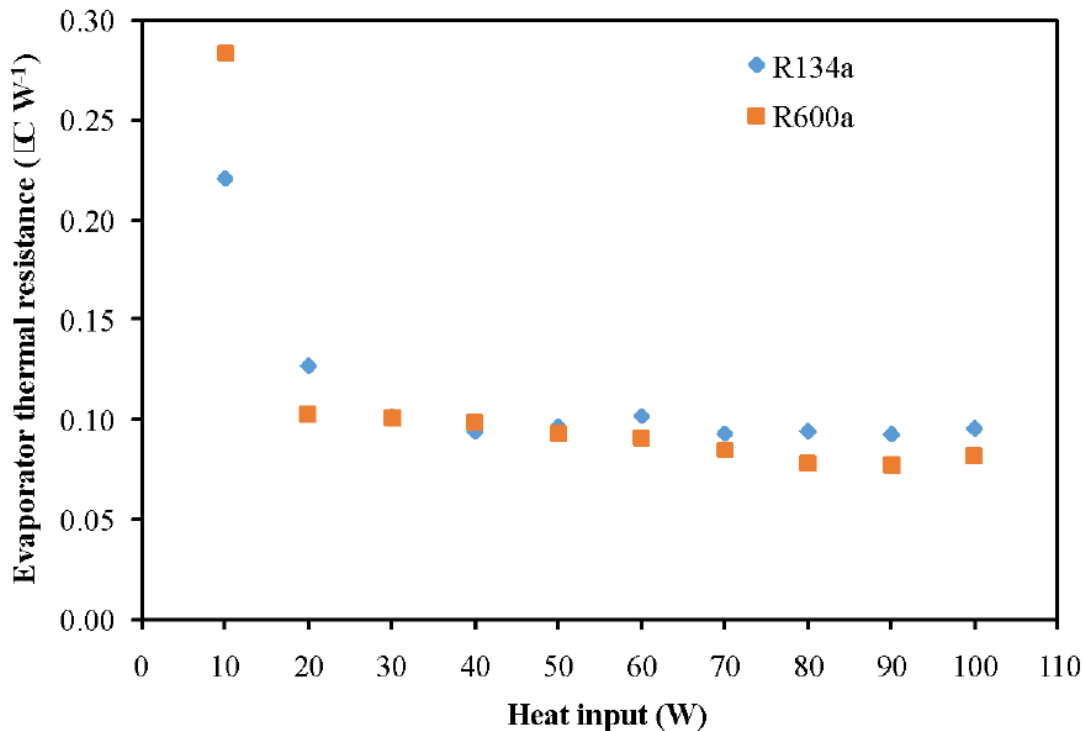


Figure 3. Thermal resistance at the evaporator section for the applied heat input

Thermal resistance is the avoiding tendency of the material or device to restrict the heat flow between the surfaces. In a THP, the thermal resistance should be very less for better heat transfer. The thermal resistance at the evaporator is shown in Figure 3, which shows a decrease in thermal resistance for the applied heat input for the THP. R600a charged THP shows higher thermal resistance for the first heat input than R134a; thereafter increasing the heat input, the thermal resistance found to be decreased (particularly for the last six heat inputs i.e., 50 W to 100 W). The evaporation characteristics between R134a and R600a charged THP depicts only a minor difference; perhaps the refrigerant R600a provides the decreased thermal resistance of 0.082 °C/W and refrigerant R134a offers slightly higher thermal resistance of 0.095 °C/W.

The thermal resistance of the condenser for the refrigerant charged THP is shown in Figure 4 for the applied heat input from 10 W to 100 W. Similarly, as evaporator thermal resistance, the condenser resistance decreases as the heat input increases. The working fluid reaches the condenser loses its vapor phase and forms liquid, hence the temperature obtained at these sections plays a vital role. The

temperature attained at the section of condenser and adiabatic is less for R600a than R134a. In this experiment, R600a reduces the thermal resistance than R134a. The mean difference between R600a and R134a charged THP is 0.013 °C/W.

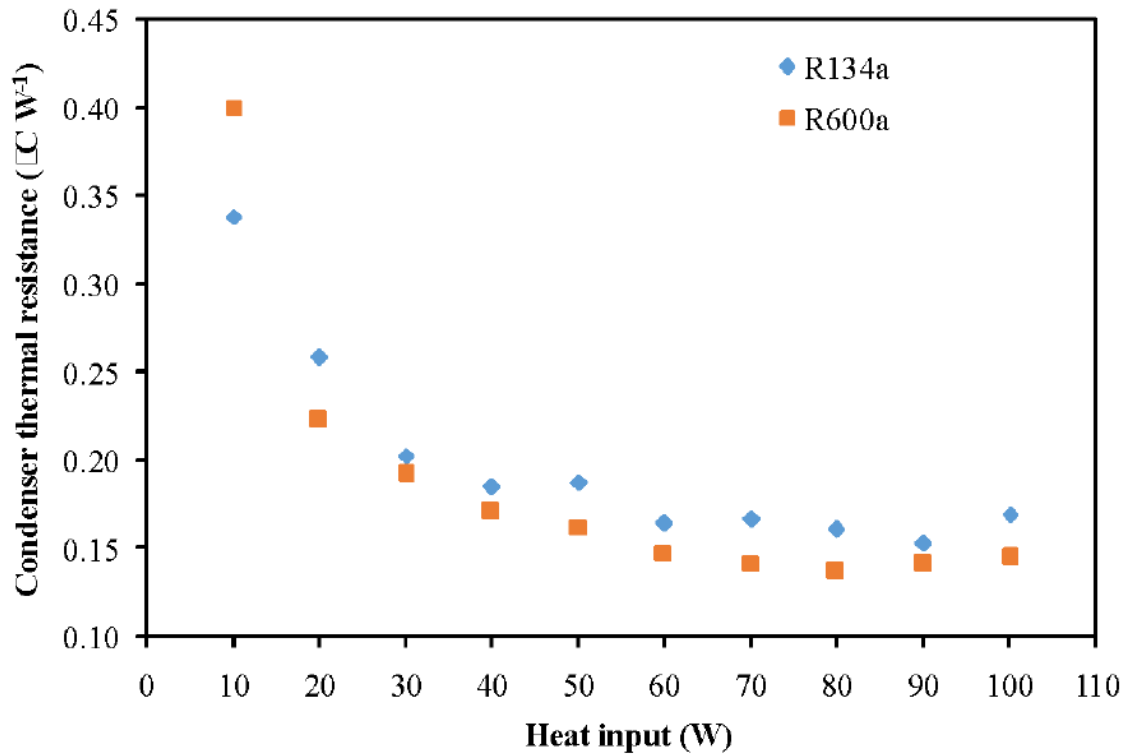


Figure 4. Thermal resistance at the condenser section for the applied heat input

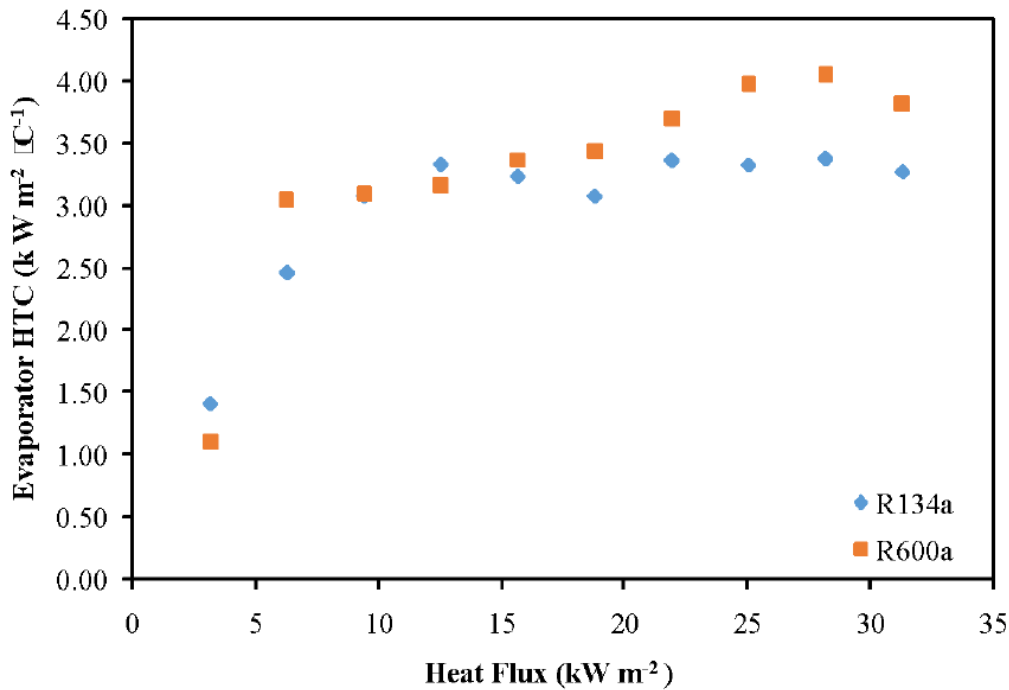


Figure 5. Heat transfer coefficient at the evaporator section for the applied heat flux

When heat is applied at the evaporator, the working fluid energizes to change its state from liquid to vapor. The formation of vapor and transfer of heat determines the heat transfer rate at the evaporator which is depicted in Figure 5. The heat transfer coefficient at the entire area of the evaporator is increased with the increase in heat flux. It is observed that the working fluid R134a shows a decrease than R600a charged THP. The heat transfer coefficient attained by R600a charged THP is 16.2% higher than R134a for the final heat input.

The cooling water circulates around the condenser section making the working fluid as the liquid forms vapor at the condenser inside the THP. The heat transfer coefficient at the condenser is represented in Figure 6, which shows the increase in trend for the supplied heat flux. When the evaporator temperature decreases, then the temperature in the condenser also decreases for the comparative analysis in THP for different working fluids. In this experiment, heat transfer at the condenser provides a promising outcome that the R600a overcomes the performance of R134a marginally in THP. The mean difference obtained between R134a and R600a charged THP is 10.7% for the condenser heat transfer coefficient.

The overall performance of the thermosyphon can be predicted by the total thermal resistance of the thermosyphon. The difference between the evaporator and the condenser to the heat input provides the total thermal resistance, which is shown in Figure 7. The difference in thermal resistance obtained between R134a and R600a is 0.028, 0.064, 0.014, 0.012, and 0.011 °C/W for the last five heat inputs, respectively, in THP. The thermal resistance shows that refrigerant R134a in THP attains a slight increase than R600a.

The refrigerant R134a is not flammable, and R600a is flammable, according to the American Society of Heating, Refrigeration and Air-Conditioning (ASHRAE) requirements. Refrigerant R134a has a higher Office of Disease Prevention (1300) than R600a, and R600a is environmentally friendly, so R600a is better. However, due to its flammable nature, safety measures must be properly maintained when using R600a as working fluid in THP.

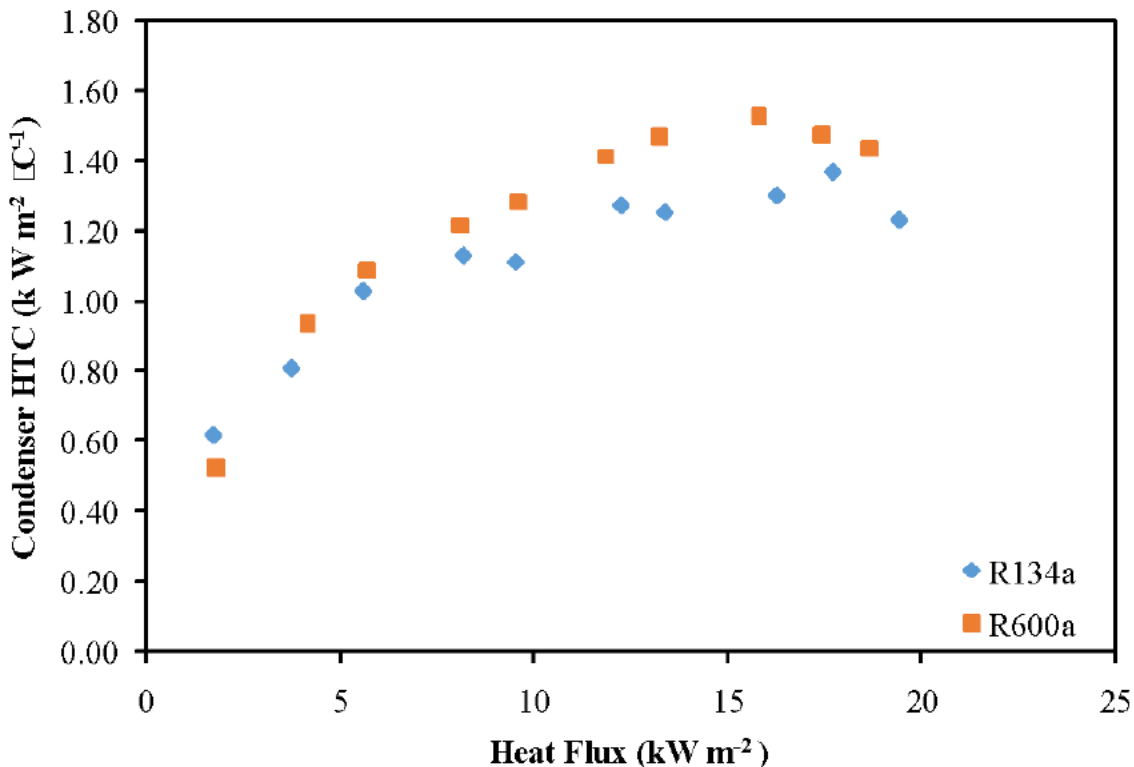


Figure 6. Heat transfer coefficient at the condenser section for the applied heat flux

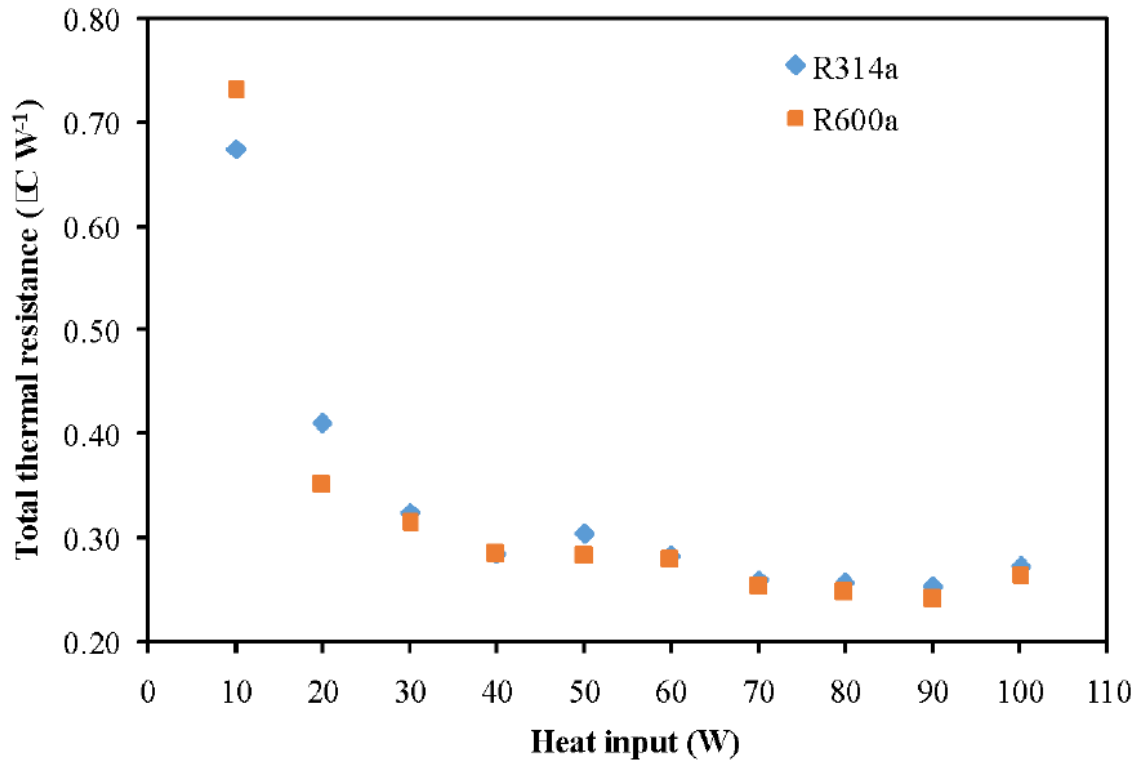


Figure 7. The overall thermal resistance of the thermosyphon for the applied heat input

Classifier-Based Approach to Predict the Outcome

Support vector machine

SVM is used to find the optimal value based on the possible outputs achieved from the experimental evaluation. This helps us classify based on learning algorithms.

Artificial neural network

ANN is an information processing method that takes in numerous inputs to be sampled and processes the inputs based on the training we provide.

Convolution neural network

CNN is a multilayered network model that manages the complex features of input data. Based on the feature extracted, the analysis is being done in this model to find the accuracy and performance level using the possible inputs we feed. This extracts the predicted accuracy level and calculates the performance based on optimality.

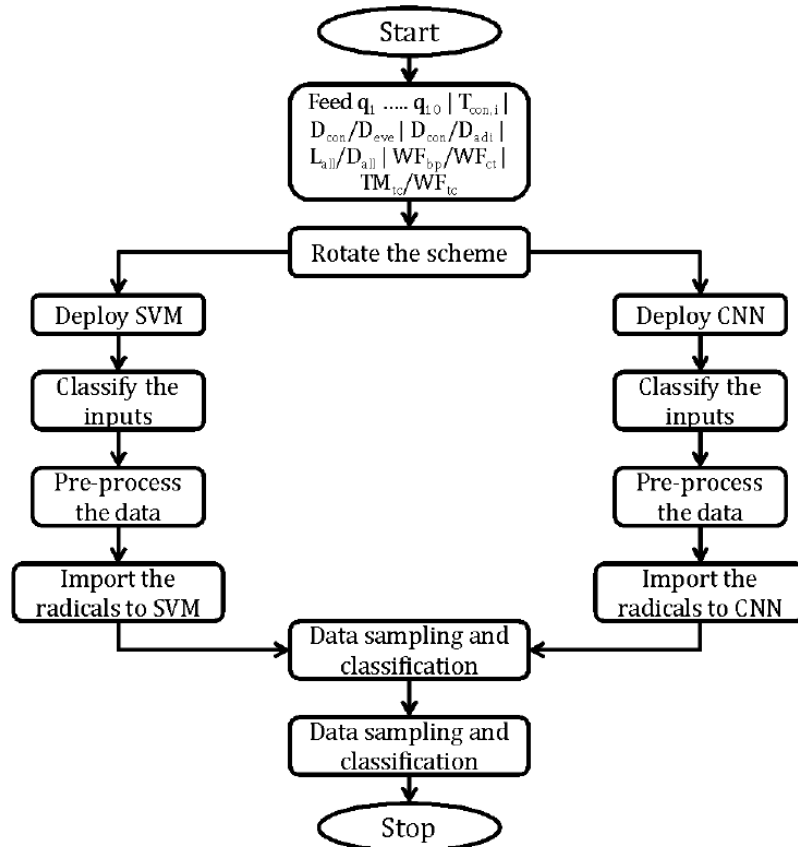


Figure 8. Block diagram of the algorithmic approach

Proposed algorithmic approach

An algorithmic approach is appended in the experimental evaluation of the refrigerants charged thermosyphon (Figure 8). The key inputs are used to compute the outcome in an algorithmic approach. Here, classifiers are used to predict the outcome theoretically when compared with the experimental results. A strong neural schema is formed with the inputs such as $Q_1, q_2 \dots q_{10} | T_{con,i} | D_{con}/D_{eve} | D_{con}/D_{adi} | D_{con}/D_{adi} | L_{all}/D_{all} | W_{Fbp}/W_{Fct} | T_{Mtc}/W_{Ftc}$ before processing the data.

The schema is fed into the classifier algorithms SVM and CNN separately. Using classifiers in this analysis will help the user strongly evaluate the process at every stage and bring out the processed output. With the inputs imposed by the researcher, the experiment would have been completed and the thermal resistance is obtained for varying inputs. The same process is automated using the machine learning approach, where the schema is considered for grade analysis. Further, to increase the complexity in preserving the original values without any disclosure, it is rotated once to create a permutation. This will enhance the mixture of varying inputs.

The input values are given to two different classifiers which can process it faster with regression. Using the SVM classifier, the inputs are split into different training points heat flux, heat input, cooling water temperature input, diameter ratio between condensers and evaporator, diameter ratio between condenser and adiabatic, ratio between overall length to the diameter of the thermosyphon, ratio between boiling temperature and critical temperature of working fluid, ratio of thermal conductivity between material and working fluid with which each stage of training points can be processed. Then the processed training points can be introduced to the sampling process. The sampled data will be compared with the experimental results to measure accuracy and efficiency.

Also, CNN, which is termed as space invariant ANN, can be introduced with the cumulative inputs, which can be segregated into various training sets of data. The real data achieved from the experimental evaluation is fed to the CNN module, and it is converted for trajectory data to be compared with the algorithmic outcome. The training sets, such as heat flux and heat input, are preprocessed in this stage, and the sampled data is taken for algorithmic convolution. The classifier refines the sampled data and produces the predicted result.

Both the results are compared with the existing accuracy level and efficiency level of the experimental evaluation with that of the algorithmic outcome. Further, SVM and CNN-based results are projected for their efficiency in this algorithm.

- a. INPUT neural scheme $Q_1, q_2 \dots q_{10} | T_{con,i} | D_{con}/D_{eve} | D_{con}/D_{adi} | L_{all}/D_{all} | W_{fbp}/W_{fct} | T_{Mtc}/W_{fct} |$ to grade analysis.
- b. ROTATE scheme to permute the input values
- c. deploy SVM and CNN classifiers to categorize the inputs and perform analytic modulation.
- d. Preprocess the data to compute manual outcomes $t_1, t_2 \dots t_8$, where t_1 to t_7 are temperature outcomes from the thermosyphon and t_8 is the outlet water temperature from the condenser.
- e. IMPORT the radicles to SVM, CNN, ANN classifiers using the medium upon which the calculation has to be done.
- f. Data sampling with the values heat flux, heat input, has to be done to moderate the results.
- g. Ratio between experimental and algorithmic thermal resistance is found and measures such accuracy, performance and efficiency are computed.

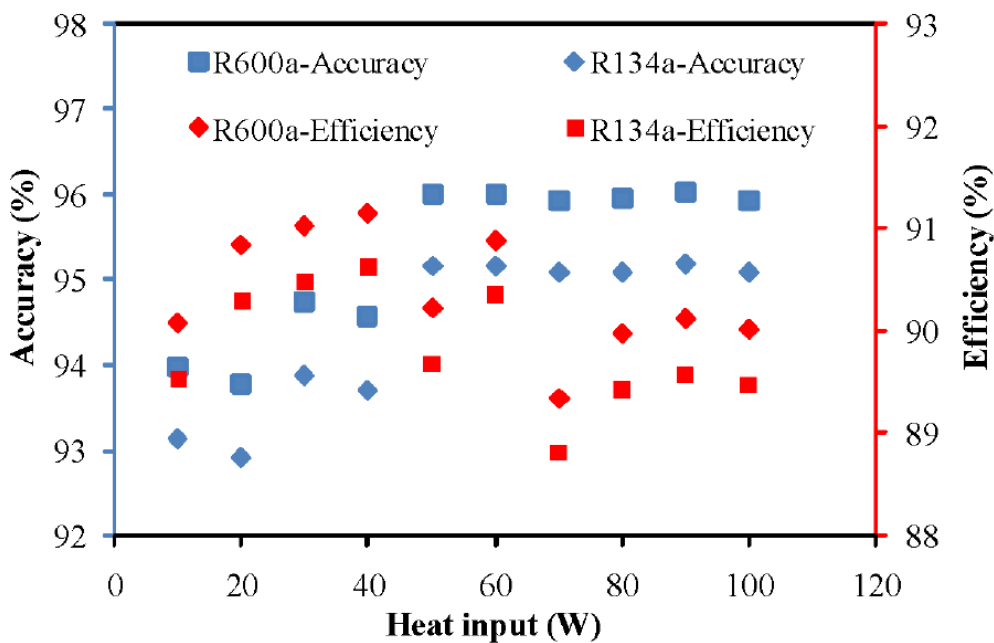


Figure 9. Accuracy and efficiency based on supporting vector machine (SVM) with the heat input

The performance metrics, including accuracy and efficiency, are measured through a support vector machine classifier method to trace the percentage of prediction. Accuracy level can be measured with the input of heat flux and predicted with the algorithmic approach to say measured accuracy. SVM method analyzes the input data heat flux, heat input, cooling water temperature input, diameter ratio between condensers and evaporator, diameter ratio between condenser and adiabatic, ratio between overall length

to diameter of thermosyphon, ratio between boiling temperature and critical temperature of working fluid, ratio of thermal conductivity between material and working fluid to various training sets and learning algorithms to prove the algorithmic accuracy level matches with the experimental thermal efficiency.

The set of training data (heat flux, heat input, cooling water temperature input, diameter ratio between condenser and evaporator, diameter ratio between condenser and adiabatic, ratio between overall length to diameter of the thermosyphon, ratio between boiling temperature and critical temperature of working fluid, ratio of thermal conductivity between material and working fluid) are labeled and fed into the algorithm to perform regression analysis and provide the predicted outcome.

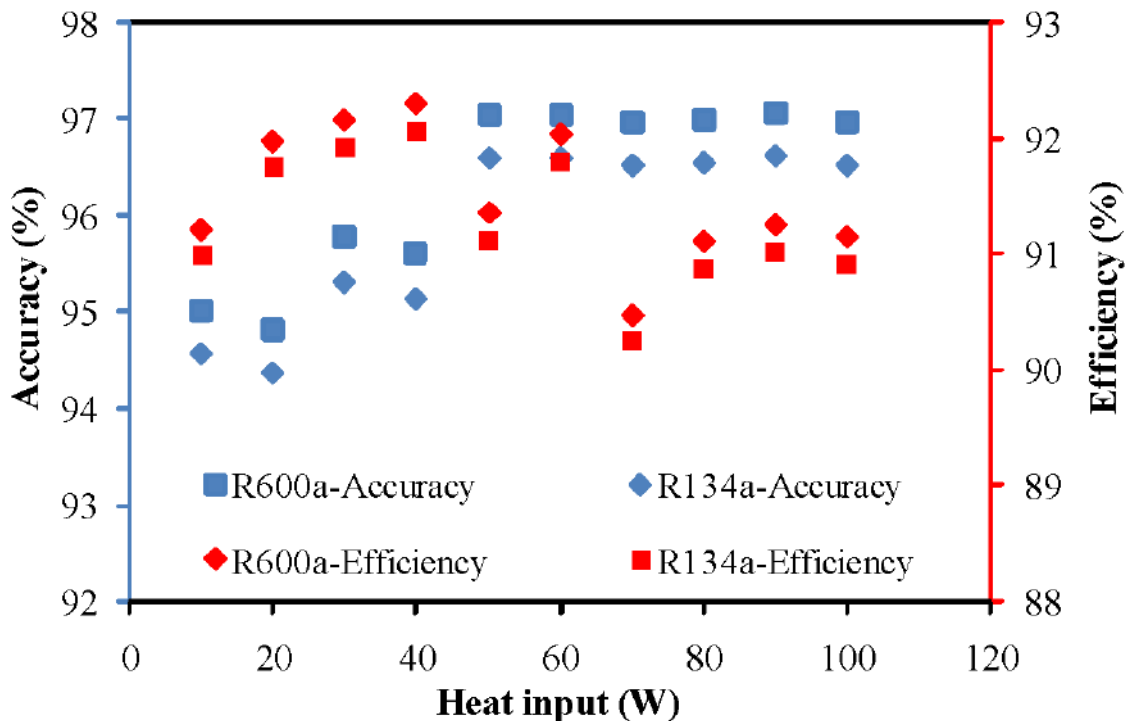


Figure 10. Accuracy and efficiency based on Convolution Neural Network (CNN) with the heat input

Using this SVM classifier, both R600a and R134a refrigerants are analyzed with multiple iterations. Figure 9 sketches the percentage of accuracy level between R600a and R134a where one is better than the other. In the same way, the performance level of both refrigerants is compared using SVM. The efficiency of the refrigerants is computed using the data analysis method and R600a is proven to be better.

When the number of iterations ($n = 5$) increases in the experimental evaluation, numerous input data are considered for analysis using the training data set and learning algorithms. Each trial carries an “n” number of inputs which will increase the thrust in analyzing the experiment in an algorithmic way. The experiment carried out uses inputs such as heat flux, heat input, cooling water temperature input, diameter ratio between condensers and evaporator, diameter ratio between condenser and adiabatic, ratio between overall length to diameter of thermosyphon, ratio between boiling temperature and critical temperature of working fluid, ratio of thermal conductivity between material and working fluid to be evaluated analytically and the accuracy, efficiency of the output arrived is measured. In this approach, the refrigerant R600a is proven to be better than the other refrigerant. Figure 10 shows that the accuracy and efficiency are 96.1 and 91.3% when compared with R134a.

The next approach imbibed over the experimental data is CNN. CNN carries complex data in the form of input, such as heat flow, the nature of working fluid and tube material, and geometric constraints, and

validates the data for future predictions. In this case, the experimental data are formed as a multilayered network to evaluate and predict its accuracy and efficiency in depth. Figure 11 depicts the efficiency and accuracy of using R600a and R134a refrigerants which stand better compared to the SVM and ANN approaches. Among the two compared refrigerants, R600a is proven to be better than R134a. Hence, the comparative analysis proves that R600a is better than the R134a refrigerant in terms of predictive accuracy and its performance in various applications.

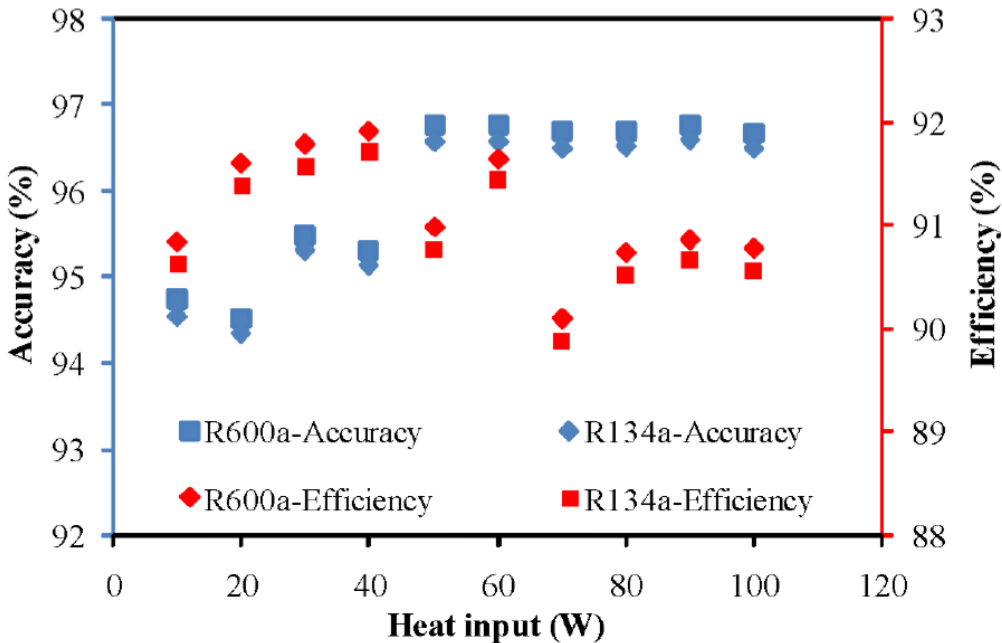


Figure 11. Accuracy and efficiency based on artificial neural networks (ANN) with the heat input

CONCLUSIONS

This study evaluated the heat transfer performance of refrigerants R134a and R600a in a thermosyphon system through experimental and machine learning approaches. The investigation yielded several significant findings regarding heat transfer performance, machine learning analysis, and comparative insights. In terms of thermal characteristics, R600a demonstrated superior performance with marginally lower thermal resistance compared to R134a, showing an overall thermal resistance difference of 2.6%. The R600a refrigerant also achieved notably higher heat transfer rates, with a 16.2% increase in the evaporator section and a 10.7% increase in the condenser section.

The machine learning component of the study revealed that among the implemented approaches (SVM, CNN, ANN), the CNN methodology proved most effective, achieving accuracy rates exceeding 95%. The CNN model demonstrated robust predictive capabilities in analyzing thermosyphon performance parameters, validating its potential for future design optimization. The comparative analysis showed that both experimental and algorithmic analyses consistently identified R600a as the more efficient refrigerant. The close alignment between experimental results and machine learning predictions validates the reliability of computational approaches for thermosyphon performance evaluation.

The study establishes a framework for future refrigerant performance assessment by combining experimental and computational methodologies. These findings suggest that R600a represents a promising alternative for thermosyphon applications while validating the effectiveness of machine learning approaches, particularly CNN, for predicting and analyzing thermosyphon performance. The successful integration of experimental and computational methods provides a valuable framework for future research in thermal system optimization.

ABBREVIATIONS

ANN	-	artificial neural networks
CNN	-	Convolution Neural Network
THP	-	Thermosyphon Heat Pipe
SVM	-	supporting vector machine

NOMENCLATURE

I	-	ammeter
A	-	area, (m ²)
D	-	diameter (mm)
H	-	heat transfer rate, (W/m ² · °C ⁻¹)
C _p	-	heat capacity, (J/kg/s)
m	-	mass flow rate, (kg/s)
R	-	resistance, (°CW ⁻¹)

Q	-	heat, (W)
q	-	heat flux, (W/m ²)
T	-	temperature, (°C)

Subscripts

adi	-	adiabatic
all	-	overall
b.p.	-	boiling point
con	-	condenser
ct.	-	critical temperature
eve	-	evaporator
i	-	inlet
in	-	input
out	-	output
o	-	outlet
sat	-	saturation
tc	-	thermal conductivity

REFERENCES

- Abas, N., Kalair, A. R., Khan, N., Haider, A., Saleem, Z., & Saleem, M. S. (2018). Natural and synthetic refrigerants, global warming: A review. *Renewable and Sustainable Energy Reviews*, *90*, 557–569. <https://doi.org/10.1016/j.rser.2018.03.099>
- Anand, R. S., Jawahar, C. P., Brusly Solomon, A., Benson, V., & Alan, A. (2020). K, K.P. Vignesh Nair, V.A. Alan, Experimental studies on thermosyphon using low global warming potential refrigerant HFE7000 and nanorefrigerant HFE7000/Al₂O₃. *Part e J. Process Mech. Eng.*, *0*, 1–11. <https://doi.org/10.1177/0954408919896690>
- Celen, A., Çebi, A., Aktas, M., Mahian, O., Dalkilic, A. S., & Wongwises, S. (2014). A review of nanorefrigerants: Flow characteristics and applications. *International Journal of Refrigeration*, *44*, 125–140. <https://doi.org/10.1016/j.ijrefrig.2014.05.009>
- Fichera, A., & Pagano, A. (2002). Neural network-based prediction of the oscillating behaviour of a closed loop thermosyphon. *International Journal of Heat and Mass Transfer*, *45*(18), 3875–3884. [https://doi.org/10.1016/S0017-9310\(02\)00095-9](https://doi.org/10.1016/S0017-9310(02)00095-9)
- Gorecki, G. (2018). Investigation of two-phase thermosyphon performance filled with modern HFC refrigerants. *Heat and Mass Transfer*, *54*(7), 2131–2143. <https://doi.org/10.1007/s00231-017-2264-4>
- Jafari, D., Franco, A., Filippeschi, S., & Di Marco, P. (2016). Two-phase closed thermosyphons: A review of studies and solar applications. *Renewable and Sustainable Energy Reviews*, *53*, 575–593. <https://doi.org/10.1016/j.rser.2015.09.002>
- Kasaeian, A., Hosseini, S. M., Sheikhpour, M., Mahian, O., Yan, W.-M., & Wongwises, S. (2018). Applications of eco-friendly refrigerants and nanorefrigerants: A review. *Renewable and Sustainable Energy Reviews*, *96*, 91–99. <https://doi.org/10.1016/j.rser.2018.07.033>
- Ma, L., Shang, L., Zhong, D., & Ji, Z. (2017). Experimental investigation of a two-phase closed thermosyphon charged with hydrocarbon and Freon refrigerants. *Applied Energy*, *207*, 665–673. <https://doi.org/10.1016/j.apenergy.2017.06.100>
- Maleki, A., Elahi, M., Assad, M. E. H., Alhuyi Nazari, M., Safdari Shadloo, M., & Nabipour, N. (2021). Thermal conductivity modeling of nanofluids with ZnO particles by using approaches based on artificial neural network and MARS. *Journal of Thermal Analysis and Calorimetry*, *143*(6), 4261–4272. <https://doi.org/10.1007/s10973-020-09373-9>
- Naresh, Y., & Balaji, C. (2018). Thermal performance of an internally finned two phase closed thermosyphon with refrigerant R134a: A combined experimental and numerical study. *International Journal of Thermal Sciences*, *126*, 281–293. <https://doi.org/10.1016/j.ijthermalsci.2017.11.033>
- Ong, K. S., Goh, G., Tshai, K. H., & Chin, W. M. (2016). Thermal resistance of a thermosyphon filled with R410A operating at low evaporator temperature. *Applied Thermal Engineering*, *106*, 1345–1351. <https://doi.org/10.1016/j.applthermaleng.2016.06.080>
- Ong, K. S., & Haider-e-Alahi, M. (2003). Performance of a R-134a-filled thermosyphon. *Applied Thermal Engineering*, *23*(18), 2373–2381. [https://doi.org/10.1016/S1359-4311\(03\)00207-2](https://doi.org/10.1016/S1359-4311(03)00207-2)

- Payakaruk, T., Terdtoon, P., & Ritthidech, S. (2000). Correlations to predict heat transfer characteristics of an inclined closed two-phase thermosyphon at normal operating conditions. *Applied Thermal Engineering*, 20(9), 781–790. [https://doi.org/10.1016/S1359-4311\(99\)00047-2](https://doi.org/10.1016/S1359-4311(99)00047-2)
- Shanbedi, M., Amiri, A., Rashidi, S., Heris, S. Z., & Baniadam, M. (2015). Thermal performance prediction of two-phase closed thermosyphon using adaptive neuro-fuzzy inference system. *Heat Transfer Engineering*, 36(3), 315–324. <https://doi.org/10.1080/01457632.2014.916161>
- Sukchana, T., & Pratinthong, N. (2016). A two-phase closed thermosyphon with an adiabatic section using a flexible hose and R-134a filling. *Experimental Thermal and Fluid Science*, 77, 317–326. <https://doi.org/10.1016/j.expthermflusci.2016.04.027>
- Zhang, H., Shao, S., Tian, C., & Zhang, K. (2018). A review on thermosyphon and its integrated system with vapor compression for free cooling of data centers. *Renewable and Sustainable Energy Reviews*, 81, 789–798. <https://doi.org/10.1016/j.rser.2017.08.011>